

## SOME ISSUES REGARDING THE ULTRA-MINIATURIZATION IN THE EDM FIELD BASED ON FINITE ELEMENT MODELLING

Daniel Ghiculescu<sup>1</sup>, Nicolae Marinescu<sup>2</sup>, George Seritan<sup>3</sup> and Liliana Popa<sup>4</sup>

<sup>1</sup>Politehnica University of Bucharest, Romania, daniel.ghiculescu@upb.ro

<sup>2</sup>Politehnica University of Bucharest, Romania, nicolae.marinescu@yahoo.com

<sup>3</sup>Politehnica University of Bucharest, Romania, george.seritan@upb.ro

<sup>4</sup>Politehnica University of Bucharest, Romania, lili.popa@yahoo.com

**ABSTRACT:** The paper deals with concentrated energy (nonconventional) machining as technological response to ultra-miniaturization challenge, namely micromachining and even nanomachining. Electrical discharge machining (EDM) has proved the opportunity to decrease the machined surfaces dimensions in nanorange (1...999 nm) at lower costs than other nonconventional machining. The finite element modelling of EDM process demonstrated the possibility that a single discharge could create a crater whose transversal dimension is lower than 999 nm.

**KEY WORDS:** electrical discharge machining, micro, nanotechnologies, finite element modelling.

### 1. INTRODUCTION

The actual major trend of ultra-miniaturization led to the development of micro-technologies generating surfaces with dimensions in the range of 1-999  $\mu\text{m}$ , and nano-technologies creating surfaces whose dimensions are situated within 1-999 nm [1].

Electrical Discharge Machining (EDM) can respond to this technological challenge due to its capacity to concentrate the discharge energy within plasma channel, whose section can be framed in micro and even nano domain. Moreover, EDM has the attribute of lower costs than other nonconventional machining (technologies with concentrated energies) like laser, ion, and electron beam machining that are able to produce surfaces required by ultra-miniaturization [2].

At micro-EDM, the discharge energy ranges between  $10^{-9} - 10^{-5}$  J. The material volume removed is  $0.05 - 500 \text{ mm}^3$ , using even a single discharge. These conditions become even more restrictive in order to crossover the threshold of nanorange.

The problem to be solved in this paper is the modelling of EDM single discharge that produces a crater whose dimensions are situated in the nano range. Nevertheless, in practice, the major difficulty to be solved is to sustain in the working gap the discharge with such low level of energy. This requires, besides the delivering of low pulse energies by EDM generator, a feed system with increments within nano range in order to maintain a stable EDM process, respectively a distance between the surfaces

of tool-electrode and machined workpiece situated in the nanorange.

### 2. SOME RELATED ISSUES FROM THE STATE OF THE ART

Obtaining dimensions in nanorange by EDM is considered one of the most advanced achievement in the this field [2], along with combination between EDM and other types of machining (hybrid machining) for high technological performances resulted from their combination [3], [4]. It was found that EDM alone has some limits for serial applications in terms of machining rate and surface quality. So, this is the reason why hybrid machining is recommended to exceed these limits [2].

The process of nano-electrical discharge machining (nano-EDM) was applied as nano-electro-machining (nano-EM) by modifying a scanning tunnelling microscopy (STM) platform, taking into account the similarities between those processes.

A tool-electrode from Platinum-Iridium (80-20%) or Tungsten 99.9% was used. The machined samples were made from gold with frontal surface levelled at atomic scale (nano-scale). The dielectric liquid used was n-decane, like at classic EDM [5], [6].

The nano-EM produced structures of nanoholes with diameters under 10 nm, using both dielectric liquid or dry medium (air) and single discharges. The finite element modelling presented below had the same approach from the point of view of discharges succession.

The disposal of obtained nanoholes is characterized by the following dimensions: the space between axes

of the nanoholes – 50 nm; the diameters of nanoholes 10 and 7.5 nm [5], [6].

The nano-EDM process is associated with some specific phenomena related to the behaviour of the dielectric liquid (n-decane) under conditions of very narrow working gap (less than 3 nm), investigated using molecular dynamics simulation. The results indicated an increase in the density of n-decane (four times) and a quasi-solid behaviour due to an effective charge transport medium between the nano-tool and the machined sample [7].

A comparison was made between wet (n-decane as dielectric liquid) and dry (air as dielectric) nano-EDM in terms of process accuracy. In the first case, the holes diameters were in average of 10 nm, and in the second case, of 7.5 nm with an increase of consistency. This is also due to some experimental observations proving that in case of wet variant the sharpening of nano-tool cannot be maintained after several discharges. In comparison, in the case of dry variant, the sharpening of electrode-tool is increased after some discharges as a result of field-induced evaporation of tool materials from the asperities of the tool tip [8].

### 3. FEM MODELLING STRATEGY AND REFERENCE EXPERIMENTAL DATA

The Finite Element Modelling of nano-EDM process of a single discharge, able to produce a crater with radius framed in the nano-domain, follows the stages depicted in fig. 1, which includes also some feedback relations to earlier stages.

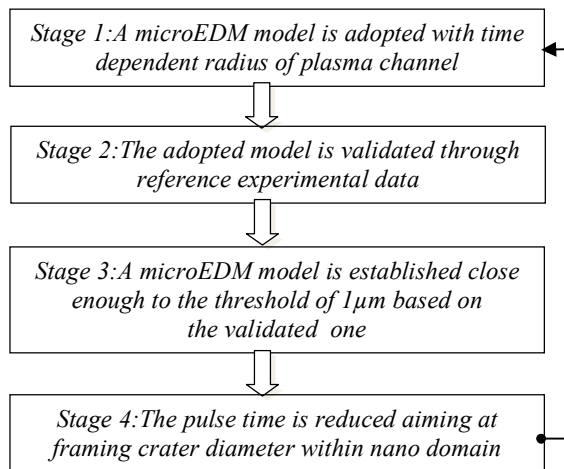


**Figure 1.** FEM stages of a process of nano-EDM

A previous study was achieved [9], comparing several models with time dependent radius of plasma channel [10], [11], [12], [13] in terms of crater dimensions produced by a single discharge, using Finite Element Modelling of micro-EDM process.

The crater dimensions obtained based on Kiyoshi Inoue’s model [14] were found closer to experimental data than the others mentioned above. Therefore, for the stage 1, the model built on the following relation, suitable for using Comsol Multiphysics was used [9]:

$$r_{ch} = 0.0014 \cdot \sqrt{t_i} \quad [m] \quad (1)$$

where:  $t_i$  is pulse time [s].

The influence of time dependent radius of gas bubble formed around the plasma channel has more reduced influence on crater dimension [15]. Consequently, a constant value model for this physical parameter was used in this current study.

The reference experimental data, obtained on X210Cr12 samples with a specialized microEDM generator and feed system with 200 nm resolution, needed to validate the adopted model in the stages 2, and 3 are presented in fig. 2, 3, 4, and 5.

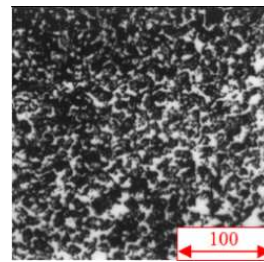


**Figure 2.** Microtopography at EDM with commanded pulses, current step,  $I=0.16A$ , pulse time,  $t_i=4 \mu s$ , pause time,  $t_o=3 \mu s$

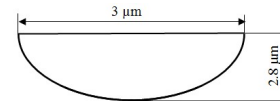


**Figure 3.** Crater profile, average dimensions at commanded pulses, current step,  $I=0.16A$ , pulse time,  $t_i=4 \mu s$ , pause time,  $t_o=3 \mu s$

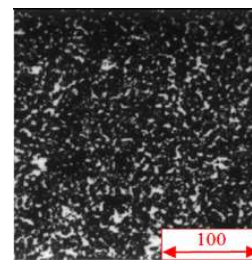


**Figure 4.** Microtopography at EDM with commanded pulses, current step,  $I=0.16A$ , pulse time,  $t_i=1 \mu s$ , pause time,  $t_o=1 \mu s$

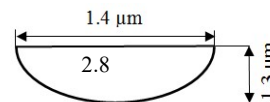


**Figure 5.** Crater profile, average dimensions at commanded pulses, current step,  $I=0.16A$ , pulse time,  $t_i=1 \mu s$ , pause time,  $t_o=1 \mu s$

### 3. FEM MODELLING OF A NANO EDM PROCESS

Comsol Multiphysics, Heat Transfer in Solids, Time Dependent variant was used for modelling the removal mechanism of nanoEDM process.

In the first stage, a 2D parametric model was created for the microEDM process, taking into account themachined geometry properties presented in fig. 6.

Name	Expression	Value	Description
lp	10[mm]	0.01 m	workpiece side length
acr	3e-6	3.0E-6	radius of initial crater
bcr	2.8e-6	2.8E-6	depth of initial crater
rbg	0.05[mm]	5.0E-5 m	radius of gas bubble
ti	0	0	pulse time - initial value
rcp	0.0014*ti^0.5	0	time dependent radius of plasma channel
a	1e-7	1.0E-7	diameter of plasma channel - initial value

Figure 6. Parameters assigned for the removal mechanism of microEDM process modelling in stage 1

The parameters assigned for the removal mechanism of microEDM model in stage 3 are presented in fig. 7.

Name	Expression	Value	Description
lp	10[mm]	0.01 m	workpiece side length
acr	1.4e-6	1.4E-6	radius of initial crater
bcr	1.3e-6	1.3E-6	depth of initial crater
rbg	0.05[mm]	5.0E-5 m	radius of gas bubble
ti	0	0	pulse time - initial value
rcp	0.0014*ti^0.5	0	time dependent radius of plasma channel
a	0.5e-7	5.0E-8	diameter of plasma channel - initial value

Figure 7. Parameters assigned for the removal mechanism of microEDM process modelling in stage 3

A 2D parameterized geometries were created as those presented in fig. 8, at initial moment (beginning of the discharge) and in fig. 9, final moment (end of the discharge).

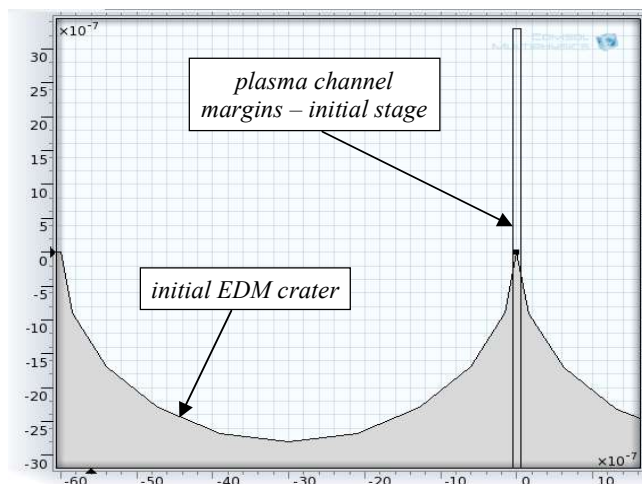


Figure 8. Parameterized microgeometry on which the single discharge was applied – initial stage

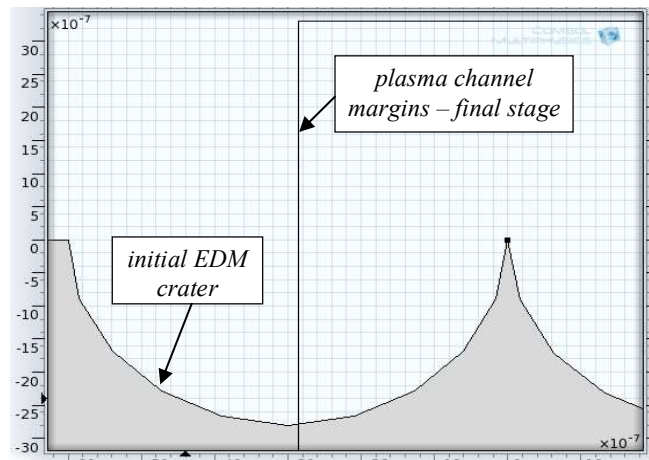


Figure 9. Parameterized microgeometry on which the single discharge was applied – final stage (pulse end)

The used material properties belong to D3 (UNS T30403), corresponding to X210Cr12 steel the material of machined samples, taken from Comsol library and completed with time dependent ones.

The meshing was a dynamic one - moving mesh along with plasma channel variation during discharge. This was achieved with up to 2976 triangular elements, average quality of 0.96 on 0-1 scale, and smaller elements in the interest zone, where a higher precision is required (fig. 10).

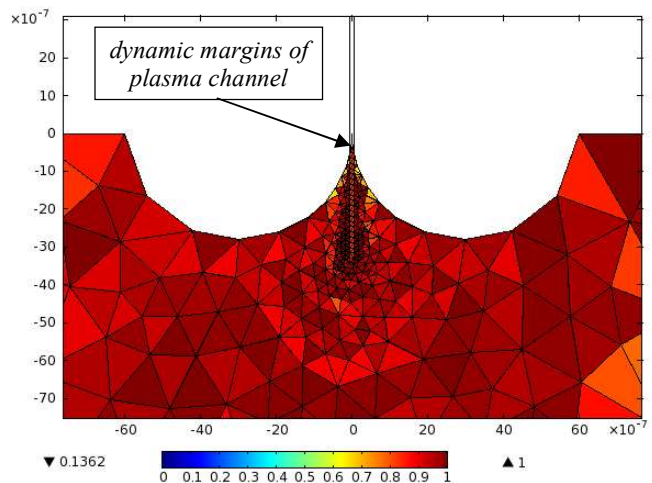


Figure 10. Dynamic mesh in interest zone with quality scale

The boundary condition on EDM spot for adopted thermal model is presented in fig. 11.

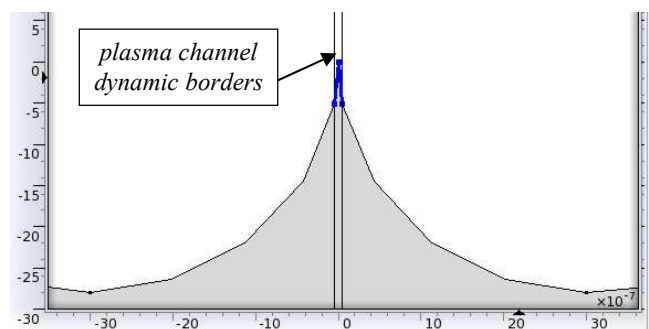


Figure 11. Temperature setup on EDM spot during pulse time

This is essentially based on Van Dijck's model of overheating the material with 200° C over boiling temperature of machined material on EDM spot in normal conditions, i.e. 3473 K in this case [15], [16].

The surface covered by the gas bubble formed around plasma channel is considered as thermal insulation (fig. 12). This lasts much longer than pulse time end, representing a natural barrier against hydraulic removal of material in liquid state during discharge and after that, the melted material being already solidified when the gas bubble collapses.

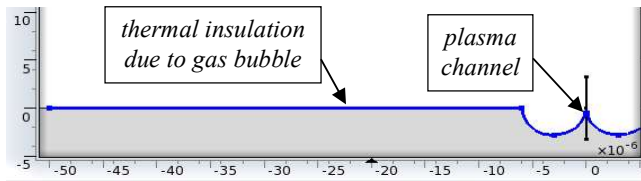


Figure 12. Thermal insulation exerted by gas bubble around plasma channel

At the periphery of the workpiece, a cooling effect is produced by immersion in dielectric liquid, at a temperature of 313 K, represented in fig. 13.

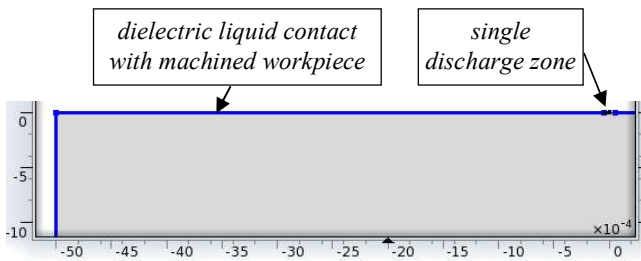


Figure 13. Cooling effect exerted by dielectric liquid

In order to obtain the crater diameter produced by single discharge under 1 μm strictly, the pulse time ( $t_i$ ) was decreased, using  $t_i$  as a sweep parameter, the Finite Element Modelling results accordingly being presented and discussed below.

#### 4. FEM RESULTS

The different temperature distribution within machined workpiece, around EDM spot, corresponding to the strategy of microEDM, and finally of nanoEDM modelling are presented below.

In fig. 14, the temperature distribution obtained after a pulse with  $t_i=4 \mu s$  is shown, respectively the material removed bordered by boiling isothermal, when the pressure suddenly drops at discharge end, accordingly to Van Dijck's model. As one can observe the coordinates  $x$  and  $y$  (radius and depth) of boiling isothermal are in agreement with reference experimental data from fig. 2 and 3 at working mode  $I=0.16 A$ ,  $t_i=4 \mu s$ . This validates the FEM model with time dependent radius of plasma channel in stage 1 of nanoEDM modelling strategy.

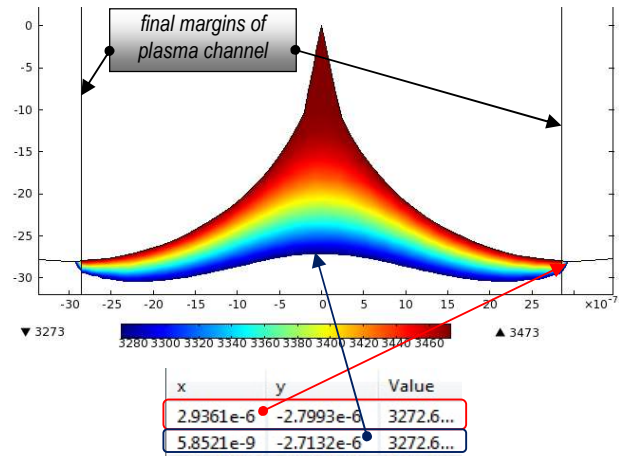


Figure 14. Temperature distribution after  $t_i=4 \mu s$  – position of boiling isothermal

Following the described above strategy, the temperature distribution obtained within machined material is presented in fig. 15 when the pulse time is decreased at  $t_i=1 \mu s$ , this corresponding to stage 3.

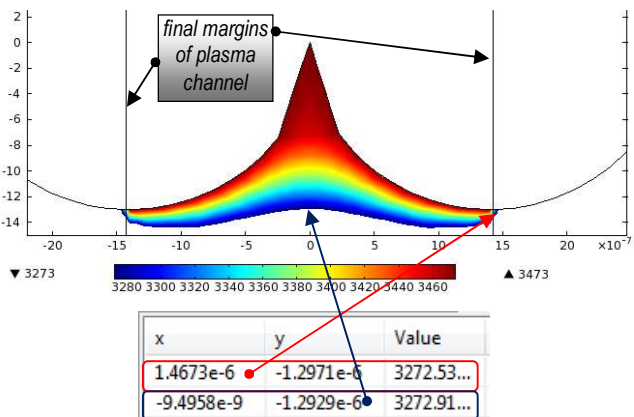


Figure 15. Temperature distribution after  $t_i=1 \mu s$  – position of boiling isothermal

As it can be noticed, the coordinates  $x$  and  $y$  (radius and depth of boiling isothermal), which determine the volume of material removed by single discharge are in agreement with crater dimensions, reference experimental data from fig. 4 and 5. Thus, the finite element model of the microprocess is validated closer to the 1 μm threshold, and was used as a basis for the following stages of nanoEDM process modelling.

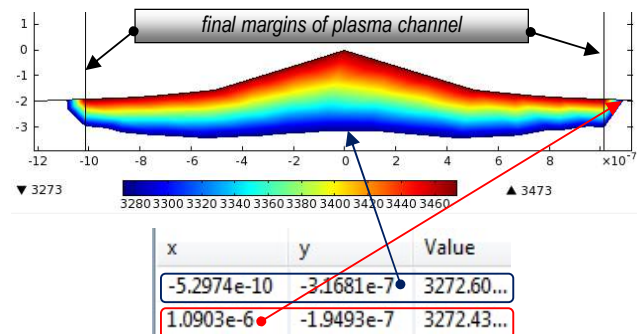


Figure 16. Temperature distribution after  $t_i=0.5 \mu s$  – position of boiling isothermal

In fig. 16, it was represented the temperature distribution within the machined sample at a first decrease of pulse time at  $t_i=0.5 \mu\text{s}$ , during final stage. As one can observe, the crater diameter obtained in this case is around  $2.18 \mu\text{m}$ .

So, the following decrease of working parameter is naturally explained, the pulse time became  $t_i=0.3 \mu\text{s}$ . Under this condition, the crater diameter was still in micrometer range since  $x$  coordinate (half of diameter) was  $0.869 \mu\text{m}$  as it is observed from fig. 17.

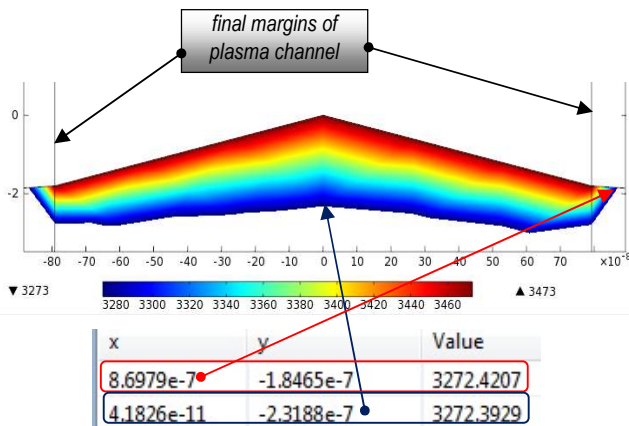


Figure 17. Temperature distribution after  $t_i=0.3 \mu\text{s}$  – position of boiling isothermal

This result justifies the next decrease of pulse time. Therefore, for  $t_i=0.1 \mu\text{s}$ , the temperature distribution after the single discharge in machined workpiece is represented in fig. 18.

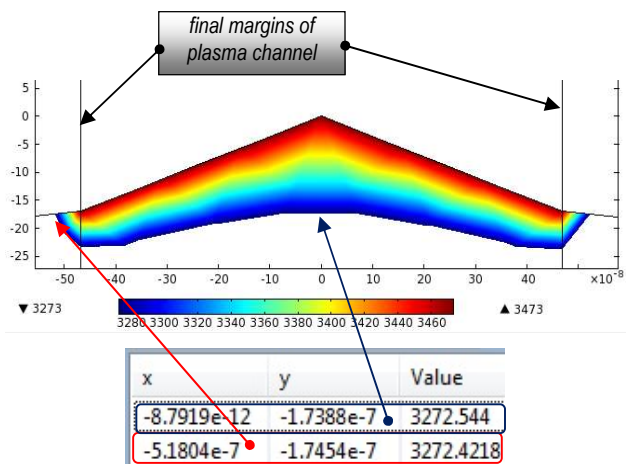


Figure 18. Temperature distribution after  $t_i=0.1 \mu\text{s}$  – position of boiling isothermal

It can be seen that crater diameter obtained for this pulse time is  $1.036 \mu\text{m}$ , still in micrometer range. Then, the decrease of pulse time is further justified.

Therefore, the pulse time is  $t_i=0.08 \mu\text{s}$ , and the position of boiling isothermal is that from fig. 19, where one can see the diameter of crater is  $940 \text{ nm}$ , framed in the nanorange.

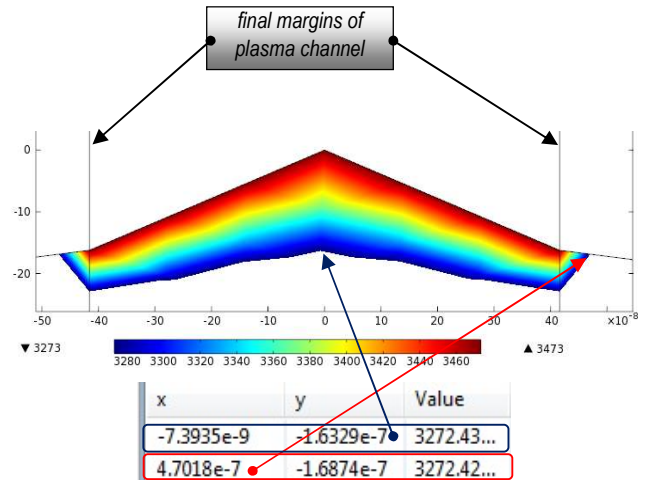


Figure 19. Temperature distribution after  $t_i=0.08 \mu\text{s}$  – position of boiling isothermal

The variation of aspect ratio, i.e. the ratio between depth (H) and diameter (D), depending on pulse time is graphically presented in fig. 20. As one can see, the aspect ratio (H/D) of the crater is visible decreased as pulse time is reduced towards framing the diameter in the nanorange.

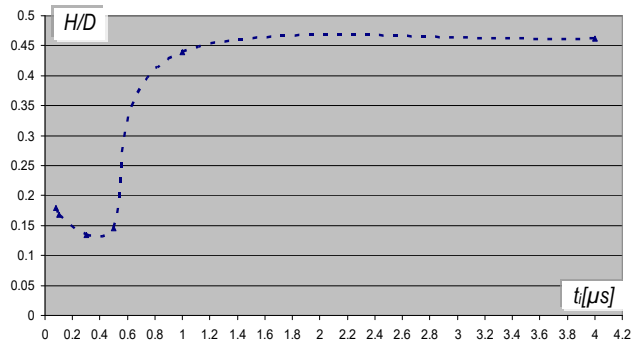


Figure 20. The aspect ration variation in respect of pulse time

The variation of crater diameter is synthetically presented in fig. 21, in parallel with H/D variation. This aims to emphasize that at low discharge energy, producing a crater diameter less than  $3 \mu\text{m}$ , the aspect ratio is suddenly decreased.

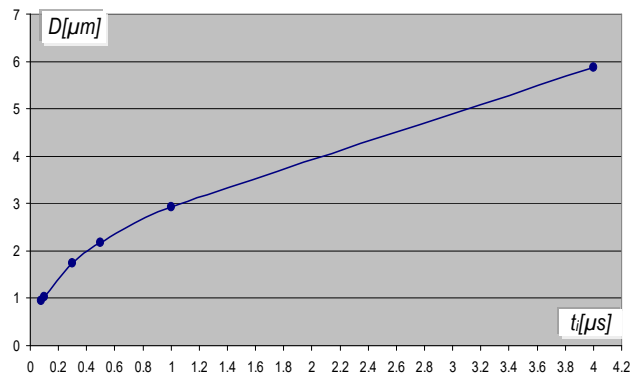


Figure 21. The crater diameter variation in respect of pulse time

## 5. CONCLUSIONS

The major and absolutely needed challenge imposed to actual technologies of machining to respond to the ultra-miniaturization reveals that the electrical discharge machining (EDM) has the characteristics to attain the threshold of the nanometer range. This machining type has the important advantage to achieve this at lower costs than other competitive technologies with concentrated energies. The researches from the state of the art proved that a very close process to EDM, i.e. nano-electrical machining by single discharge can generate surfaces whose dimensions are less than 10 nm.

These advances in the field justifies the effort of modelling the nanoEDM process in order to explain the specific material removal mechanism and thus to early build a base for optimization of working parameters aiming at appropriate decrease of discharge energy. FEM results pointed out that an EDM process having pulse time lower than  $0.08\mu\text{s}$ , discharge current less than 0.1 A, and a feed increment in nanometer range could be able to descend the generated dimensions within a high alloyed steel under the nanometer threshold.

## 6. ACKNOWLEDGEMENT

Researches financed through the projects: Joint Applied Research Project supported by MEN-UEFISCDI, project no. PN-II-PT-PCCA-2013-4-0236, Contract no. 222/2014.

## 7. REFERENCES

1. Masuzawa, T., Tonshoff, H. K., Three-dimensional micromachining by machine tools, *Annals of the CIRP*, Vol. 46, No. 2, p. 621-628, (1997).
2. Jahan, M.P., et al. *Electrical Discharge Machining (EDM), Types, Technologies and Applications*, Nova Publishers, New York, USA, (2015).
3. Khatri, B. C., Rathod, P., Valaki, J. B., Ultrasonic vibration-assisted electric discharge machining: A research review, *Proceedings of the Institution of Mechanical Engineers, Part B, Journal of Engineering Manufacture*, March, pp. 1-12, (2015).
4. Chavoshi, S. Z., Luo, X., Hybrid micro-machining processes: A review, *Precision Engineering*, 41, pp.1-23,(2015).
5. Malshe, A.P., Virwani, K.R., Rajurkar, K.P., Deshpande, D., Investigation of nanoscale electro machining (nano-EM) in dielectric oil, *Annals of the CIRP – Manufacturing Technology*, Vol. 54, pp. 175–178,(2005).
6. Jahan, M. P., Malshe, A. P., Rajurkar, K. P., Experimental investigation and characterization of nano-scale dry electro-machining, *Journal of Manufacturing Process*, 14 (4), pp. 443–451, (2012).
7. Kalyanasundaram, V., Virwani, K.R., Spearot, D.E., Malshe, A.P., Rajurkar, K.P., Understanding behavior of machining interface and dielectric molecular medium in nanoscale electro-machining, *CIRP Annals*, Vol. 57, Issue 1, pp. 199-202, (2007).
8. Jahan, M. P., Virwani, K. R., Rajurkar, K. P., Malshe, A. P., A comparative study of the dry and wet nano-scale electro-machining, *Procedia CIRP*, Vol. 6 pp. 626 – 631, (2013).
9. Ghiculescu, D., Marinescu N.I., Nanu S., Ghiculescu Daniela, Some aspects of finite element modelling of micro-EDM and ultrasonic EDM with time dependent radius of plasma channel, *Nonconventional Technologies Review*, No. 2, June, pp. 30-35,(2013).
10. Patel, R., Barrufet, A., Eubank, T., DiBitonto, D. Theoretical models of the electrical discharge machining process-II: the anode model. *Journal of Applied Physics*, Vol. 66, pp. 4104-4111, (1989).
11. Shuvra, D., Mathias, K., Klocke, F., EDM simulation: finite element-based calculation of deformation, microstructure and residual stresses. *Journal of Materials Processing Technology*, Vol.142, pp. 434-451, (2003).
12. Marafona, J., Chousal, J.A.G., A finite element model of EDM based on the Joule effect, *International Journal of Machine Tools and Manufacture*, Vol. 46, No. 6, pp. 595-602, (2006).
13. Salonitis, K., Stournaras, A., Stavropoulos P., Chryssolouris, G., Thermal modelling of the material removal rate and surface roughness for die-sinking EDM, *International Journal of Advanced Manufacturing Technology*, Vol. 40, No. 3-4, pp. 316-323, (2009).
14. Inoue, K., *Fundamental of Electrical Discharge Machining*, Society of Non – Traditional Technology, Tokyo, (1977).
15. Ghiculescu D., Marinescu N., O. Alupeii, M. Căruțașu, Some issues regarding finite element modelling of micro-electrical discharge machining aided by ultrasonics, *Key Engineering Materials*, Vols. 651-653, pp. 683-688, (2015).
16. Van Dijck, F., Snoeys, R., Theoretical and Experimental Study of the Main Parameters Governing the Electrodischarge Machining Process, *Mecanique*, Vol. 301-302, pp. 9-16. (1975).